Chemical Standards, NPL, who provided the sample of alumina and Dr J. L. Henshall of Oxford University who supplied the silicon carbide.

References

1. P. L. PRATT, 4th International Conference on Fracture, *Fracture* 3 (1977) 909.
2. J. L. HENSHALL, D. J. ROWCLIFFE and J. W. EDINGTON, 4th International Conference on Fracture, *Fracture* 3 (1977) 875.
3. E. A. ALMOND and B. ROEBUCK, *Metals Technol.* 5 (1978) 92.
4. J. J. PETROVIC, R. A. DIRKS, L. A. JACOBSON and M. Cr. MENDIRATTA, *J. Amer. Ceram. Soc.* 59 (1975) 177.
5. J. L. CHERMANT and F. J. OSTERSTOCK, *J. Mater. Sci.* 11 (1976) 1939.

Received 3 January
and accepted 31 January 1978.

E. A. ALMOND
B. ROEBUCK
Division of Materials Applications,
National Physical Laboratory,
Teddington, Middlesex, UK

Formation of a DO_{19} phase in zirconium–aluminium martensites

Of the several intermetallic phases that form in the zirconium–aluminium system, the one richest in zirconium occurs around the composition Zr_3Al and has the $L1_2$ structure [1, 2]. Recently, Schulson and Graham [3] have examined in detail the formation of this phase in near-stoichiometric alloys through the peritectoid reaction:

$$Zr + Zr_2Al \rightarrow Zr_3Al.$$

It is also possible, in more dilute alloys, to make this phase precipitate in a martensitic or a non-martensitic α-Zr(Al) matrix by ageing in the $\alpha + Zr_3Al$ phase field after quenching from either the beta or the alpha phase regions.

While studying the evolution of Zr_3Al in a martensitic matrix an interesting result was obtained on the basis of certain preliminary observations made on a Zr–4.6 wt % Al alloy and this is briefly reported in this note. The alloy was made in a non-consumable arc furnace in the usual manner, using sponge zirconium and pure (99.99%) aluminium. The finger obtained was homogenized at 1150° C (which corresponded to beta-solutionizing) and was subsequently water quenched to induce the martensitic transformation. Chemical analysis showed that the alloy contained 14 at. % (4.6 wt %) aluminium, 1100 p.p.m. oxygen, 500 p.p.m. carbon and 60 p.p.m. nitrogen.

Transmission electron microscopy revealed that the martensite produced in this alloy was of the dislocated lath type and that the structure appeared to consist of a single phase (Fig. 1). However, selected area diffraction patterns (Fig. 2), obtained from various regions of the samples examined, invariably showed two sets of spots. Those belonging to the first set could be indexed in terms of a disordered h c p structure, having lattice parameters approximately equal to those of alpha zirconium. But the spots of the second set could not be so indexed. These spots, though sharp and well formed, were in general fainter and appeared only at the mid-points of straight lines joining the directly transmitted spot to those spots of the first set that were associated with planes $\{h\,k\,i\,l\}$ for which l was an even integer. The likely reasons for the occurrence of these faint spots could be (i) double diffraction, (ii) an extremely fine scale precipitation of the equilibrium Zr_3Al phase during quenching and (iii) ordering of the α-Zr(Al) solid solution. A systematic examination of the extra spots in various reciprocal lattice sections (obtained from diffraction patterns at various orientations of the foils with respect to the electron beam) showed

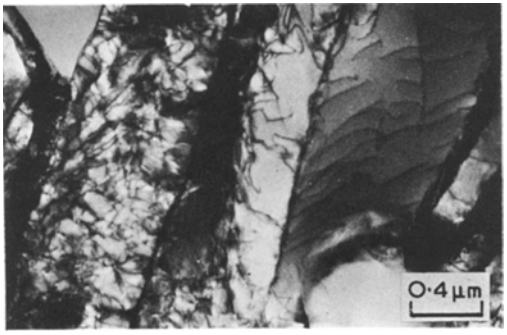

Figure 1 Single phase dislocated lath martensite structure of the beta quenched alloys.

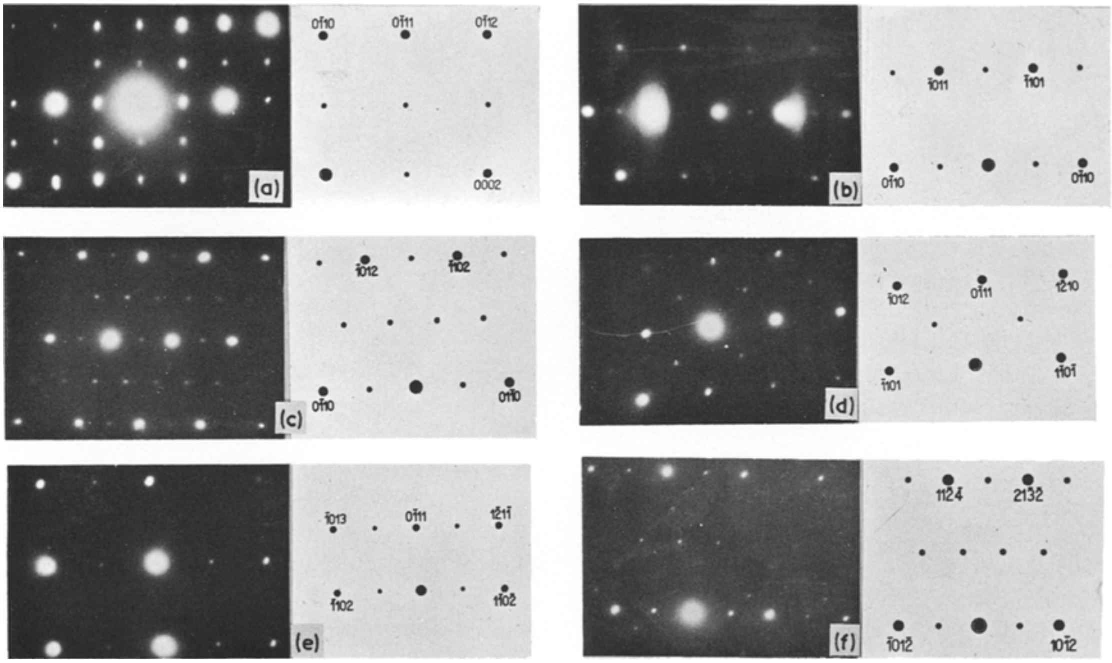

Figure 2 Selected area diffraction patterns corresponding to several reciprocal lattice sections of the DO_{19} structure. (a) Zone axis: $[2\,\bar{1}\,\bar{1}\,0]$. (b) Zone axis: $[2\,\bar{1}\,\bar{1}\,3]$. (c) Zone axis: $[4\,\bar{2}\,\bar{2}\,3]$. (d) Zone axis: $[1\,0\,\bar{1}\,1]$. (e) Zone axis: $[5\,\bar{1}\,\bar{4}\,3]$. (f) Zone axis: $[\overline{10}\,14\,\bar{4}\,3]$. The indices of the zone axes and of the spots in the keys are in terms of the disordered h c p structure. The larger circles represent the fundamental reflections while the smaller stand for either superlattice or forbidden reflections.

that only a few of these could be accounted for solely on the basis of double diffraction. It was also found that not all spots of the second set matched with one or other of the reciprocal lattice sections corresponding to the $L1_2$ structure. Furthermore, the interplanar spacings associated with many of these spots, calculated by using the appropriate values of the microscope camera constant, were found to be inconsistent with respect to the possible "*d*" spacings of the equilibrium Zr_3Al phase (whose reported lattice parameter is 4.374 A° [2]). For instance, spots associated with interplanar spacings larger than that of the $\{1\,0\,0\}$ planes in Zr_3Al were noticed. These observations suggested that the appearance of the second set of spots was due to an ordering of the α-Zr (Al) solid solution. The observed locations of these spots and the calculated interplanar spacings associated with these were consistent with the formation of a superstructure whose unit cell edges (A_1, A_2, C) were parallel to those of the disordered h c p solid solution (a_1, a_2, c), the axis transformation matrix being

$$\begin{bmatrix} 2 & 0 & 0 \\ 0 & 2 & 0 \\ 0 & 0 & 1 \end{bmatrix}.$$

An identical geometrical relationship is known to exist between the unit cells of the DO_{19} and the h c p structures [4, 5]. In view of this, it could be inferred that the observed diffraction patterns were indicative of a h c p → DO_{19} ordering reaction during quenching. This was further checked by plotting several DO_{19} reciprocal lattice sections (using an axial ratio equal to half that for alpha zirconium) and comparing these with the observed diffraction patterns. It was found that each pattern matched with one or other of these reciprocal lattice sections, showing that a DO_{19} phase (whose unit cell volume was approximately four times that of the disordered solid solution) did exist in the beta quenched alloy. Using the expression for the structure factor for the DO_{19} structure [6] it was also found that in each diffraction pattern the spots of the first set corresponded to fundamental reflections and those of the second to superlattice reflections.

The occurrence of the ordering reaction during the process of quenching suggested that its kinetics were fast. However, in view of the hypostoichiometry of the alloy and the extremely short period of time it could spend at temperatures where one could expect a reasonable atomic mobility, it was likely that the quenched alloy was only partially ordered. This state of order could correspond either to an imperfect ordering of the entire solid solution (continuous ordering), leading to a low value of the long range order parameter, or to a dispersion of small ordered regions (which could have even a high degree of order) in the disordered solid solution. The latter situation was found to prevail. Though the quenched structure appeared single phase in bright field, careful dark-field imaging, using superlattice reflections, showed the presence of a uniform distribution of DO_{19} microdomains in a disordered matrix (Fig. 3). The average size of these islands of order was about 50 Å. These observations implied that while the diffraction spots belonging to the second set were associated with the superlattice reflections of the DO_{19} phase, those of the first set were due to the hcp as well as the fundamental DO_{19} reflections. The fact that most of these spots did not show any appreciable splitting suggested that the interplanar spacings of the $\{h\,k\,i\,l\}$ planes in the hcp phase were very nearly equal to those of the $\{2h\ 2k\ 2i\ l\}$ planes in the DO_{19} phase.

In a binary A–B alloy the DO_{19} structure, like the $L1_2$ structure, is usually associated with the A_3B (or AB_3) stoichiometry. It was likely, therefore, that the observed ordered phase had a composition near Zr_3Al. It appeared that this was a transition phase – a structural variant of and a precursor to the equilibrium $L1_2$ phase. It is pertinent to mention in this context that these two ordered structures have a remarkable structural similarity and are homeotect. The arrangement of atoms in the basal plane of the DO_{19} structure is identical to that in the (1 1 1) plane of the $L1_2$ structure. Furthermore, the atomic arrangement in any two successive basal planes in the former is identical to that in any two consecutive (1 1 1) planes in the latter. The only difference between the two structures lies in the manner the third successive layer is stacked. Ordered, close packed layers of atoms (of composition A_3B) stacked in the sequence 010101... result in the DO_{19} structure while the sequence 012012... generates the $L1_2$ structure.

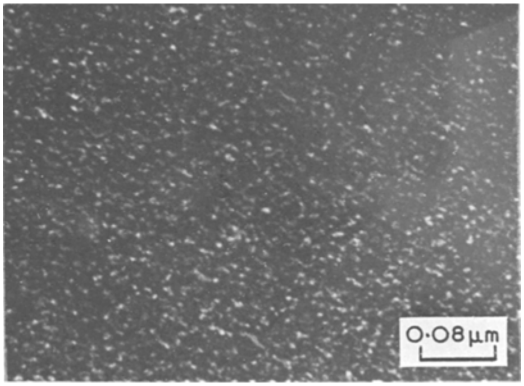

Figure 3 Ordered microdomains imaged with a DO_{19} superlattice reflection.

References

1. D. J. McPHERSON and M. HANSEN, *Trans. ASM* 46 (1954) 354.
2. M. POTZSCHKE and K. SCHUBERT, *Z. Metallk.* 53 (1962) 548.
3. E. M. SCHULSON and D. B. GRAHAM, *Acta Met.* 24 (1976) 615.
4. M. J. MARCINKOWSKI, "Electron Microscopy and Strength of Crystals" (Interscience, New York, 1963) p. 333.
5. J. W. CHRISTIAN and P. R. SWANN, "Alloying Behaviour and Effects in Concentrated Solid Solutions" (Gordon and Breach, New York, 1965) p.105.
6. P. MUKHOPADHYAY, *Trans. Ind. Inst. Metals* 29 (1976) 185.

Received 3 January
and accepted 31 January 1978.

P. MUKHOPADHYAY
V. RAMAN
S. BANERJEE
R. KRISHNAN
Metallurgy Division,
Bhabha Atomic Research Centre,
Trombay, Bombay 400 085, India